DREXEL INSTITUTE OF TECHNOLOGY

Wave Propagation Research Center

Philadelphia, Pennsylvania

October 24, 1969

Office of University Affairs
National Aeronautics and Space Administration
Washington, D. C.   20546

Attention: Technical Reports Officer
             Code Y

Subject: Annual Status Report covering the period September 1, 1968
           to September 1, 1969 on NASA Grant NGR 30-004-013

Gentlemen:

During this reporting period we have made progress in the following areas:

I.   Computer Analysis

MCDIT-21, developed under our first year's grant, has been
utilized to analyze nineteen shell impact problems. These analyses
consisted of determining the effect of shell thickness ratios and boundary
condition functions on the response of cylindrical and conical shells. A
modified version of MCDIT-21 has been developed; this modification
reduces by one-half the computational time.

II.   Experimental Evaluations

A photodiode projectile velocity measurement system has been
designed and built. In addition, conclusions have been reached regard-
ing material property evaluations and the utilization of strain gages
and force gages.

III.   Experimental and Analytical Comparisons

We found the measured elastic wave velocities in cylindrical shells
with thickness ratios of 0.052, 0.133, and 0.286 to be essentially the
plate wave velocity. This experimental result agrees with the wave
velocity used in our thin shell theory. Furthermore, we found our thin
shell theory adequately predicts the pulse magnitude and shape of longi-
tudinal and circumferential strains in the three cylindrical shell
specimens.

IV.   Publications

Nine papers have been submitted or accepted during this reporting
period.

V.   General

       This grant has wholly or partially supported three faculty,
four graduate students and two undergraduate students.

                              Sincerely yours,

                              Richard W. Mortimer
                              Principal Investigator
                              Assistant Professor
                              Department of Mechanical Engineering

RWM:hc

Attachments

DREXEL INSTITUTE OF TECHNOLOGY
Wave Propagation Research Center
Philadelphia, Pennsylvania

October 24, 1969

ANNUAL REPORT

FOR

WAVE PROPAGATION IN STEPPED AND JOINED SHELLS

Richard W. Mortimer
Pei Chi Chou
Joseph L. Rose

September 1, 1968 to September 1, 1969

TABLE OF CONTENTS

I. COMPUTER ANALYSIS

A. Solutions

MCDIT-21 computer code, developed under the first year's grant has been utilized to analyze the following shell impact problems. Package 12 of this Code was used for the cylindrical shells and Package 13 for the conical shells.

1. Cylindrical Shells

a. Variation of Thickness Ratios

i. The response of a cylindrical shell, with thickness ratios (h/R) of 0.1, 0.05, and 0.01 subjected to a longitudinal velocity impact prescribed as a step function, was obtained. The pertinent conditions were:

$\dot{u}$ (o,t) (Longitudinal velocity) = 1.0

$\dot{\psi}$ (o,t) (Rotational velocity) = 0

Q (o,t) (Transverse shear) = 0

The results of these computations are shown in Figs. 1 a, b, and c for longitudinal stress, moment, and transverse shear stress, respectively. Also included in these figures are the results obtained from a modified membrane theory. This membrane theory differs from the classical membrane theory in that transverse shear deformation is included, yielding governing equations of the following form

$$u'' - \frac{\ddot{u}}{c_p^2} = - - -$$

$$w'' - \frac{\ddot{w}}{c_s^2} = - - - \tag{1}$$

This system of equations (1) was also solved by MCDIT 21 subjected to the boundary conditions:

$\dot{u} = 1.0$

$Q = 0$

-3-

ii. The response of a cylindrical shell, with h/R of 0.1 and 0.5 subjected to a radial velocity impact prescribed as a step function, were solved. The boundary conditions were:

$$\dot{w}\,(o,t)\ (\text{radial velocity}) = 1.0$$

$$N_x\,(o,t)\ (\text{longitudinal stress}) = 0$$

$$M_x\,(o,t)\ (\text{moment}) \qquad = 0$$

The results of these computations are shown in Figs. 2 a, b, and c for longitudinal stress, moment, and transverse shear stress, respectively. Again, results obtained by solving the modified membrane equations are included in these figures.

b. Variation of Rise Times for Ramp Boundary Conditions

i. The response of a cylindrical shell (h/R = 0.1), subjected to longitudinal velocity impact prescribed as initially a ramp followed by a constant value, was solved. Solutions were obtained for three values of rise times. The boundary conditions used in conjunction with Problem Package 12 were:

$$\dot{u}\,(o,t) = \begin{cases} 1\ (t/t_{Rise}) & ; \ o \leq t \leq t_{Rise} \\ 1 & ; \ t_{Rise} \leq t \end{cases}$$

$$\dot{\psi}\,(o,t) = 0$$

$$Q\,(o,t) = 0$$

Figures 3 a, b, and c show the longitudinal stress, moment, and transverse shear distributions, respectively, for values of dimensionless t_{Rise} = 0.1, 0.5, and 1.0. For comparison, each figure includes the distribution obtained by using the step boundary condition.

ii. The response of a cylindrical shell (h/R = 0.1) subjected to radial velocity impact was solved subject to the following prescribed boundary conditions:

$$\dot{w}(o,t) = \begin{cases} 1 \ (t/t_{Rise}) & ; \ o \le t \le t_{Rise} \\ 1 & ; \ t_{Rise} \le t \end{cases}$$

$$N_x(o,t) = 0$$

$$M_x(o,t) = 0$$

Again, the response was computed for each of the three values of dimensionless t_{Rise} = 0.1, 0.5, and 1.0. Figures 4 a, b, and c show the resulting distributions of longitudinal stress, moment, and transverse shear stress, respectively. The corresponding results for a step input are also included in the figures.

2. Conical Shell (semi-vertex angle of 45°)

a. Variation of Thickness Ratios

The response of a conical shell, with h/R ratio of 0.1 and 0.05 subjected to longitudinal velocity impact prescribed as a step function, was solved. The boundary conditions utilized for this problem were:

$$\dot{u}(s_o,t) = \cos \alpha = 0.707$$

$$\dot{w}(s_o,t) = -\sin \alpha = -0.707$$

$$\dot{\psi} = 0$$

Figures 5 a, b, and c show the meridional stress, moment, and transverse shear stress distributions, respectively. The solution to the same problem using the equations from the modified membrane theory are also included in these figures. The boundary conditions used for the membrane solution were

$$\dot{u}(s_o,t) = .707$$

$$\dot{w}(s_o,t) = -0.707$$

b. Variation of Rise Times for Ramp Boundary Conditions

   i. The response of a conical shell with $h/R_o = 0.1$ was

   computed for the boundary conditions

$$\dot{u}\,(s_o,t) = \begin{cases} .707\;(t/t_{Rise}) & ;\;\; o \leq t \leq t_{Rise} \\ \\ .707 & ;\;\; t_{Rise} \leq t \end{cases}$$

$$\dot{w}\,(s_o,t) = \begin{cases} -.707\;(t/t_{Rise}) & ;\;\; o \leq t \leq t_{Rise} \\ \\ -.707 & ;\;\; t_{Rise} \leq t \end{cases}$$

$$\dot{\psi}\,(s_o,t) = 0$$

   Figures 6 a, b, and c include the results of these calculations

   together with the corresponding jump response.

B. Modification of MCDIT 21 Computer Code

   The present MCDIT 21 computational procedure is based on the method

of characteristics. The integration of the governing equations is

performed along the characteristic lines in the physical plane (see

Figure 7). The computational procedure, as it exists in MCDIT 21, pro-

ceeds from the leading characteristic along a left-running characteristic

to the boundary (x = o). For example, the first computation solves for

all variables at point B (Figure 7), since all the variables are known

at point A from the initial conditions. The computation then proceeds

to the left running characteristic CDE where the variables at point D

then at point E are calculated; the variables at the points along FG are

calculated next, followed by the points on line HI. This procedure is

continued until sufficient points are calculated for the user. The points

at which the variables are calculated are included in the shaded triangle

shown in Figure 7. The reason for calculating this entire field is that

the user can present his results as either spatial or temporal distributions.

However, much computer time is wasted by this procedure when we desire to compare analytical results with experimental results obtained from transducers located at specific locations along the structure. In order to reduce the computer time for this application of MCDIT-21 a modified version of the computer code has been completed and is described in the next paragraph.

For the purpose of describing the essence of the modification to MCDIT-21, we will assume that a variable of interest (e.g. strain) has been measured experimentally at a particular location (x_1), and from this experimental information we know the time duration of the pulse with which we wish to compare. We superimpose this time duration onto the physical plane, shown as PQ in Figure 8. The computational procedure begins as described above; variables at B are calculated first, then variables along the left-running characteristic CE are calculated. The modification to the code is initiated with the calculations along the left-running characteristic FG. Instead of calculating the variables along the entire characteristic line (including the point on the boundary), we halt the calculations at point G and move to the next left-running characteristic and calculate the variables at the points I and J. This procedure is followed until the calculations at Q have been completed. In order to obtain the same time duration (PQ) in the original MCDIT-21 code we would calculate the variables at all points in the triangle OMN, whereas in the modified version we need to calculate the variables at only those points in the strip OEQM (shown as the shaded region in Figure 8). This modified version of MCDIT-21 yields a considerable saving in computer time.

II. EXPERIMENTAL EVALUATIONS

A. Projectile Velocity Measurement System

The purpose of this system is to measure the velocity of a projectile, or impacter, prior to impact with the test specimen. Figure 9 is a schematic diagram of this system, consisting of a pendulum impacter, photodiodes, and light source, while Figure 10 is a photograph of the actual system. The pendulum impacter includes the Pendulum Arm, Shell Impacter, and Cardboard Tab.

The velocity of the impacter is determined by letting the Cardboard Tab pass through a light signal emitted by a light source to a photodiode oscilloscope. The photodiode system (Fig. 9) is set up as follows. Three photodiodes are monitored on the oscilloscope. The oscilloscope is adjusted in such a way that, when the leading edge of the Cardboard Tab interrupts the light signal to the first photodiode, the scope is triggered and initiates a single sweep. On passing through the second and third photodiodes the Cardboard Tab interrupts each light signal which, in turn, interrupts the sweep on the oscilloscope. At that instant the screen is photographed and thus captures the interruption of the signal of all three photodiodes. The time for the Tab's leading edge to pass from the second to the third photodiode is determined by measuring the distance between interruptions on the photograph, and then relating this distance to units of time by the oscilloscope sweep setting. A Tektronix timemark generator was used to calibrate the time-base before and after each test.

The velocities of the aluminum shell impacters, being used in these experiments, have been obtained by the system described above, and are listed in the following table.

Spec. No.	h in.	$\frac{h}{R}$	l_1 in.	l_2 in.	Vel. ft/sec.
T-1	.052	.052	29-3/8	32-5/8	13.4
T-13	.133	.133	29-9/32	32-12/32	13.5
T-14	.286	.286	29-9/32	32-13/32	13.0
T-15	.375	.462	29-1/4	32-1/2	13.5

All specimens are 6061T6 aluminum with a proportional limit of 40,000 PSI. They are 96.4% pure aluminum.

B. Material Properties

The decision has been made to utilize the static handbook or manufacturers listed properties for the materials tested in the low speed impact tests. The reason for this is the fact that the strain rate effect does not appreciably alter the elastic region of the stress-strain curve (especially at our low velocity of impact) of the material. In addition, the technique of obtaining meaningful dynamic stress-strain properties for the experiment under consideration is still not explicitly developed; the method of translating data from a dynamic test into precise properties is not a simple exercise. For example, wave propagation effects should be considered in establishing the dynamic properties, thus strain and strain-rates vary with position of specimen.

In the future, when we study plastic wave propagation we will need the dynamic properties of the material since a valid yield criteria will be based on the proportional limit and the non-plastic portion of the stress-strain is highly affected by the strain-rate.

These conclusions were based on material found in Goldsmith's book, IMPACT, and conversations with Dr. N. Cristescu and the Materials Testing Laboratory at Westinghouse.

C. Strain Gages

Below is listed a series of statements regarding our findings for the use of strain gages, adhesives, and surface preparation. The list of references are found at the end of this Section.

1. Frequency Response

    a. J.M. Krafft[1], in reviewing the frequency response of wire resistance strain gages, states that these gages are excellent for the study of wave propagation.

2. Strain Gages

    a. We are presently using 1/8" long, open-faced, epoxy-backed strain gages (Automation Industries) for our aluminum shell studies, however, Automation Industries is dropping smooth epoxy-backed gages. For future tests we will use the gage described in (b) below.

    b. After trying many gages for our air gun steel bar impact studies, we have been most satisfied with the Micro-Measurement gage, EA-XX-125AD-120; this gage is an open-faced general purpose gage with polyimide backing. The XX denotes the temperature compensation (13 for aluminum and 06 for steel). The E-option provides a polyimide encapsulation to protect the gage surface. Many people believe that better transducer accuracy can be obtained by avoiding this option, however, we have noted no difference in experimental results. Option S is available with solder dot terminals on the tabs; we have found that the smallest quantity of solder on the tabs produced the most repeatable results. We have decided to use this Micro-Measurement gage for our future aluminum shell studies.

REFERENCES

1. J.M. Krafft, "Instrumentation for High Speed Strain Measurement," Met. Soc. Conf., Vol. 9, RESPONSE OF METALS TO HIGH VELOCITY DEFORMATION.

2. Private communication between Joe Rose, Dick Schaller, Dr. C.C. Perry, Vice President of Vishay Intertechnology and author of "Strain Gage Primer."

3. Private communication between Joe Rose, Dick Schaller and L. Weymouth of BLH and Clyde Moyer of Photolastic Inc.

4. Private conversation between Joe Rose and Jack Marshall of NOL.

5. Rand, Yang, Marshall, "Dynamic Compression of Strain-Rate Materials," NOL-TR 65-10, 1965.

6. Yang, Rand, Marshall, "Stress Wave Propagation in Strain-Rate Sensitive Materials," NOL-TR 65-11, 1965.

7. P.P. Keough, "Pressure Transducer for Measuring Shock Wave Profiles," DASA-1414, SRI, 1963.

8. Personal communications between J. Rose, R. Mortimer and L. Seamens, (SRI).

9. James F. Bell, "An Experimental Study of Instability Phenomena in the Initiation of Plastic Waves in Long Rods," printed in MECHANICAL BEHAVIOR OF MATERIALS UNDER DYNAMIC LOADS, edited by Springer-Verlag New York, Inc.

10. G.L. Filbey, Jr., Ph.D. Dissertation, The Johns Hopkins University (1961).

11. G.L. Filbey, Jr., TR No. 8, U.S. Army BRL Contract No. DA-36-034-21X4992, 509-ORD-3104RD, The Johns Hopkins University (1961).

12. G.L. Filbey, Jr., Proc. Symposium on Structural Dynamics Under High Impulsive Loading, 147 (1963).

13. W.J. Halpin, O.E. Jones, and R.A. Graham, "A Submicrosecond Technique for Simultaneous Observation of Input and Propagated Impact Stresses, Symposium on Dynamic Behavior of Materials.

3. Adhesives

   a. We have found the GA-2 epoxy to be unsatisfactory for our application. In addition, the installation process for this epoxy is difficult due to required clamping pressures.

   b. We are presently using Certified Eastman 910 or GA-1 with epoxy backed, open-faced gages for the aluminum shell studies. Certified Eastman 910 was recommended for our application by Perry[2], Weymouth[3], and Moyer[3]. In addition, Marshall[4] (NOL) recommended the Certified Eastman 910 adhesive with Micro-Measurement polyimide backed gages for our impact application. Marshall also emphasized the importance of proper surface preparation, especially removal of contaminants. This gage and adhesive were used by Marshall in obtaining the results published in Refs. 5 and 6.

   c. Perry[2] recommended M Bond-600 adhesive if the Certified Eastman 910 fails. This M Bond-600 adhesive requires clamping pressure and oven curing, but for higher impact velocities it may be the only acceptable adhesive. However, Marshall claims that Certified Eastman 910 should be adequate in the higher impact velocity region as well.

4. Surface Preparation

   a. We have found the 400 grit paper to be most appropriate for aluminum and the 240 grit paper best for steel.

   b. We have found that gage waterproofing is necessary because of our humidity problems in the laboratory, as well as protecting the gage from dirt and contaminants.

D. Force Gages

A decision to postpone the use of force (or stress) gages has been made. Briefly, the reasons are two-fold. First, impedance mismatch between imbedded transducer and material is still a problem which can cause wave reflection and wave inter-action at the interface yielding incorrect readings. Second, the experiment must be one-dimensional for the transducer to give proper results. Any straining in a direction other than that of principal axis of the transducer distorts the geometry of the transducer yielding incorrect readings. These conclusions were obtained by personal communications and literature search (see Refs. 7-13).

III. EXPERIMENTAL AND ANALYTICAL COMPARISONS

Our main research emphasis in the last half of this reporting
period has been the comparison of experimental and analytical responses
for cylindrical shells subjected to axial impact. Three aluminum shells
with thickness ratios (h/R) of 0.052, 0.133, and 0.286 were impacted by
shells of identical material properties and cross-sectional geometry.
The velocity of the impacting shell was measured by a photodiode
system (see Section II.A); this velocity measurement stipulated our
boundary conditions for the analytical solutions. Strain gages measuring
longitudinal strain were mounted on the shell at distances of 1", 3",
7.5", 15", 20", and 25" from the impacted end; three gages were mounted
120° apart at the 3" location to determine simultaneity of impact. .
Strain gages used to measure circumferential strain were mounted at 7.5"
and 15" from impacted end. With the responses monitored from these
gages we were then able to compare theoretical and experimental wave
velocities and theoretical and experimental strain pulses.

Before describing the specific results from each of the three
cylindrical specimens we will discuss, briefly, the data acquisition
and test procedure. The first item to be determined was the impact
simultaneity (e.g. planeness of wave) of each test. Our procedure for
determining the simultaneity of each test was to mount three longitudinal
strain gages, 120° apart, at the 3" location. By monitoring these
three gages a record of simultaneity was recorded for each test on an
oscilliscope. A typical oscilliscope picture showing the three traces
is shown in Figure 13 . Simultaneity was considered acceptable for a
test if there was less than 3 microseconds difference between the arrival
times at the three gages and if there was less than 5 percent difference

in the three strain pulse magnitudes. Two oscilloscopes were available
to record the gage traces (a total of ten) as it was necessary to run
four series of tests for each specimen; one scope was used to determine
simultaneity and the second scope was used to record the traces of two
or three (if chopped mode used) of the remaining gages. For each series
of tests at least three sets of acceptable data (good simultaneity) was
recorded. Repeatability of the tests was found to be very good. The
strain gages and adhesives used in these tests are described in Section
II-C.

The strain data was recorded on an oscilloscope through the use of
an Ellis BAM-1B bridge amplifier tuned to a frequency response of 100 KC.
Adjustments on the Ellis amplifier and the oscilloscope amplifier
permitted strain scalings of 400 µin/in/division for longitudinal strain
and 200 µin/in/division for circumferential strain. In several tests
a scope amplifier chop mode was used to record simultaneously three strain
traces. The oscilloscope, set on single sweep, was triggered when the
pendulum impacter contacted the shell specimen. To insure the accuracy
of the time scale on our oscilloscope traces a time-mark generator was
used. The procedure for superimposing the time marks on the oscilloscope
traces was to double expose the Polaroid film by changing the channels
on the oscilloscope amplifier immediately after the strain test was
completed and photographing the time marks.

A. Wave Velocity Comparison

In this Section the comparison of measured and analytical
longitudinal wave velocities is presented. The experimental wave velocities
are obtained between succeeding strain gages mounted at different axial
locations along the specimen shell (see Table I for location of
longitudinal strain gages). The wave velocity between two strain gages

is obtained by dividing the distance between the gages by the difference

in arrival times of the pulse as monitored by each gage. The results,

as presented in Table I, are the average measured wave velocities based

on at least three tests. Since the wave velocity used in the theoretical

analysis is the plate velocity $\sqrt{\dfrac{E}{\rho(1-\nu^2)}}$ each experimental wave velocity

is presented as a ratio of the experimental velocity to the plate

velocity. Also included in Table I are the properties of the three

cylindrical shell specimens tested. It is estimated that the experi-

mental velocities we obtained are within $\pm$ 3% experimental error. This

error is mainly introduced in the measurement of the difference in arrival

times between two gages even though a 6X Edscorp pocket comparator for

analyzing the oscilloscope photographs was used. Typical oscilloscope

traces showing longitudinal strains at various axial locations are shown

in Figs. 14 and 15; Figs. 16 and 17 contain other typical strain traces.

With the realization that for the three specimens tested the ratio

of dilatation velocity to plate velocity is 1.15 and the ratio of bar

velocity to plate velocity is 0.94 it can be concluded that the longi-

tudinal pulses in specimen T-1 and T-13 travel with the plate velocity

(within experimental accuracy) along the entire length of the specimens.

However, it appears that the longitudinal pulse in the thickest specimen

(T-14) is initially traveling faster than plate velocity but after it

has traveled two or three diameters down the shell its velocity is the

plate velocity, also.

B. Comparison of Longitudinal Strains

In this section the comparisons between experimental and

analytical longitudinal and circumferential strains are presented in

Figs. 18, 19, and 20, for each of the three specimens. The comparisons

for the longitudinal strains are shown at 3 and 7.5 inches from the

impacted end and the circumferential strain comparisons are shown at 7.5

inches. The analytical results shown in Figs. 18, 19, and 20 were obtained

by using Package 12 of MCDIT-21 subject to the boundary conditions

$$\dot{u}\ (o,t) = \begin{cases} \dfrac{\text{velocity of pendulum impacter}}{2} & ;\ 0 < t < t_{\text{duration}} \\[2ex] 0 & ;\ t_{\text{duration}} < t \end{cases}$$

$$Q\ (o,t) =\quad 0$$

$$\dot{\psi}\ (o,t) =\quad 0$$

The magnitude of the prescribed longitudinal velocity, $\dot{u}$ (o,t), is

equal to one half the measured velocity of the pendulum impacter (see

Section II-A for impacter velocity for each specimen) and the duration

of pulse, t_{duration}, is specified as the time for the wave to travel two

lengths of the shell impacter. All computations were performed on an

IBM 360-65; a mesh size of 0.05" was used for each problem.

Figure 18 contains the strain comparisons for Specimen T-1

(h/R = 0.052). The analytical and experimental longitudinal strains

at 3" and 7.5" are shown in Figure 18(a) and 18(b) While the circumferential

results at 7.5" are shown in Figure 18(c). For this Specimen two analytical

results are shown in each Figure; one based on a step boundary condition

for $\dot{u}$(o,t) (see above) and the other based on a boundary condition for

$\dot{u}$(o,t) which involved a ramp of 4 μsecs followed by a constant velocity

(same velocity as used in step boundary condition) for the remainder of

pulse duration. The step analytical results produce good pulse magnitude

and shape agreement with experiment, although the experimental longitudinal

strain peaks trail the analytical peaks due to the initial finite rise

times of the experimental strain.

-17-

Figure 19 contains the strain comparisons for Specimen T-13 (h/R = 0.133). The analytical results presented for this comparison are based on the step boundary condition for $\dot{u}(o,t)$. The analytical results produce good pulse magnitude and shape agreement with the experimental strains. However, the longitudinal and circumferential strain peaks trail those obtained analytically; this effect is more pronounced in Specimen T-13 than in T-1.

Figure 20 contains the longitudinal strain comparisons at 1", 3", and 7.5" and the circumferential strain comparison at 7.5". Again we note good agreement for pulse magnitude and shape with the experimental strain peaks trailing those obtained analytically.

Based on the above strain comparisons we can conclude that the thin shell theory used in MCDIT-21 adequately predicts the longitudinal and circumferential strain pulse magnitudes and shapes for the three shell specimens. However, we believe comparisons should be made at the 15" and 20" locations in order to determine the extent of the trailing of the experimental stress peaks. Hopefully, these additional comparisons would aid in further ascertaining the applicability of thin shell theory to thicker shells.

IV. PUBLICATIONS AND REPORTS

Listed below are the publications, presentations, and reports written to-date which have been supported by NASA Grant NGR 30-004-013.

1. "Analysis of Transient Structural Response by the Method of Characteristics," P. C. Chou, presented at the Symposium on Transient Loads," NASA-LRC, November 1967.

2. "Analysis of Axisymmetrical Motions of Cylindrical Shells by the Method of Characteristics," P. C. Chou, AIAA Journal, Vol. 6, No. 8, August 1968, pp. 1492-1497.

3. "MCDIT-21 - A Computer Code for One-Dimensional Elastic Wave Problems," R. Mortimer and J. Hoburg, NASA CR-1306, April 1969.

4. "The Classification of Partial Differential Equations in Structural Dynamics," P. C. Chou and R. Perry, presented at AIAA Structural Dynamics and Aeroelasticity Specialists Conference, New Orleans, La., April 1969.

5. "A New Theory for Conical Shells Amenable to Sharp Impact Analysis," R. Mortimer, presented at 2nd Canadian Congress of Applied Mechanics, University of Waterloo, Canada, May 1969.

6. "A General Linear Theory of Thick Shells of Revolution," R. Mortimer, P. C. Chou and H. Kiesel, DIT Report 340-3, June 1969.

7. "Elastic Impact of a Conical Bar," R. Schaller and R. Mortimer, submitted to 5th Southeastern Conference for Theoretical and Applied Mechanics for presentation and publication in Conference Proceedings.

8. "A Unified Linear Theory for Shells of Revolution," R. Mortimer and P. C. Chou, Final Draft being prepared for submission to AIAA Journal.

9. "MCDIT-21 - A General Purpose Computer Program for Solving One-Dimensional Elastic Wave Problems," R. Mortimer and J. Hoburg, submitted to AIAA/ASME 11th Structures, Structural Dynamics, and Materials Conference.

V. GENERAL

A. Personnel Involvement

2 - Faculty; Drs. P. C. Chou and R. W. Mortimer

1 - Instructor; Mr. Joseph Rose

4 - Graduate Students; Messrs. Blum, Carleone, Perry, and Schaller

2 - Undergraduate Students: Messrs. Fliss and Raisch

Of the four graduate students listed above, two are Ph.D. students, one is presently taking his Ph.D. Candidacy Examination, and one is a M.S. student who will take his Ph.D. Examination in Spring 1970. Mr. Perry has just completed his Ph.D. thesis, Mr. Schaller expects to complete his thesis in June 1970. These two theses have been partially supported by this grant.

B. Lectures

The Wave Propagation Research Center sponsored a series of ten lectures by Dr. N. Cristescu (University of Bucharest) on the topic of Dynamic Plasticity. The Center is sponsoring another series of seminars starting October 1969 on the topic of Wave Propagation. Speakers who have accepted to-date include Dr. George Herrmann (Northwestern University), Dr. Walter Herrmann (Sandia), Dr. George Duvall (Washington State University) and Dr. H. Hopkins (University of Manchester, Great Britain).
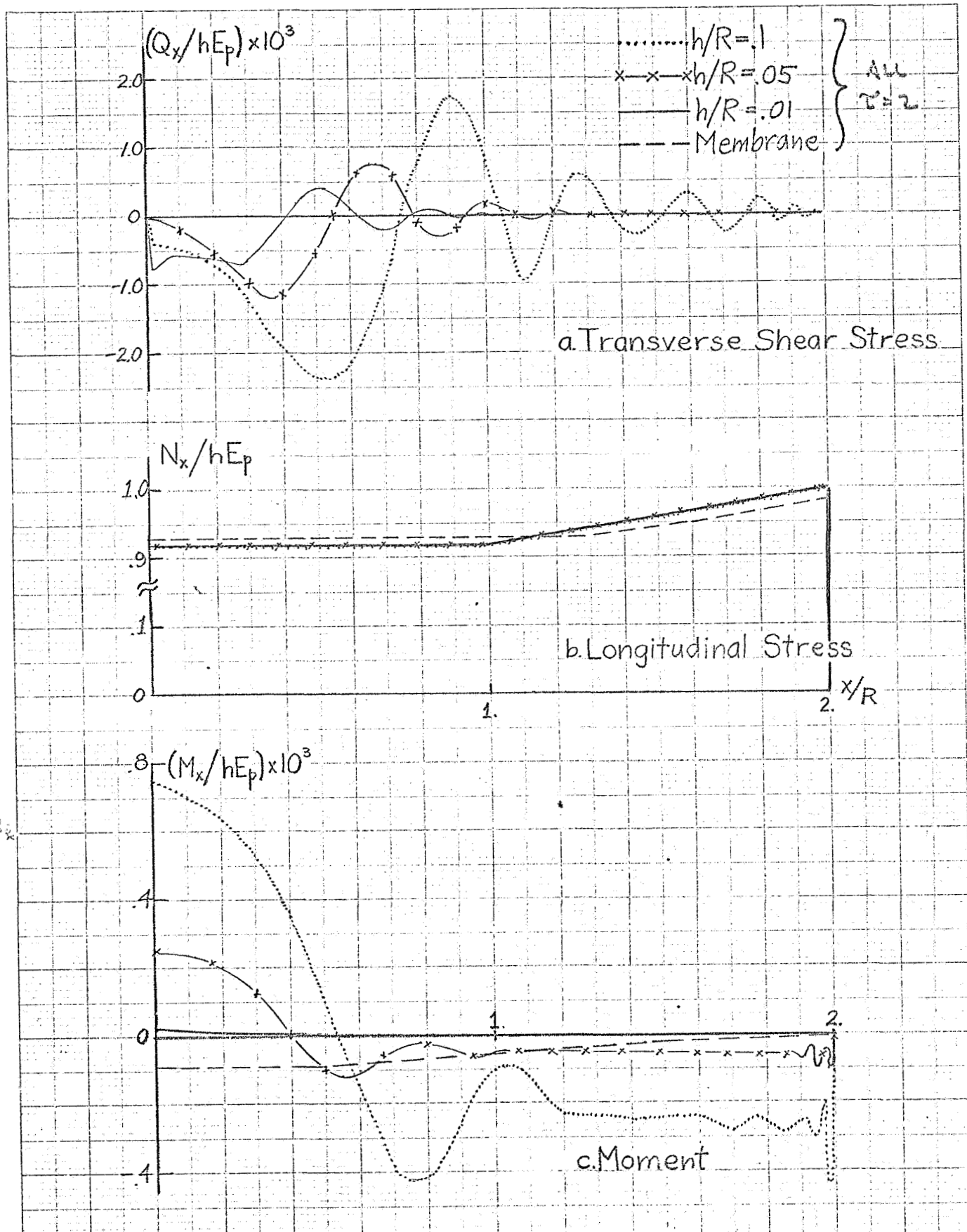
a. Transverse Shear Stress

b. Longitudinal Stress

c. Moment

Fig. 1. Cylindrical Shell
Subjected to
Longitudinal Velocity Step Impact

a. Transverse Shear Stress

b. Longitudinal Stress

c. Moment

Fig. 2. Cylindrical Shell
Subjected to
Radial Velocity Step Impact

Legend:
- $h/R = .1$
- $h/R = .05$
- Membrane

ALL $\tau = 2$

Axis labels:
- Q_x/hEp
- $(N_x/hEp) \times 10$
- $(M_x/hEp) \times 10^2$
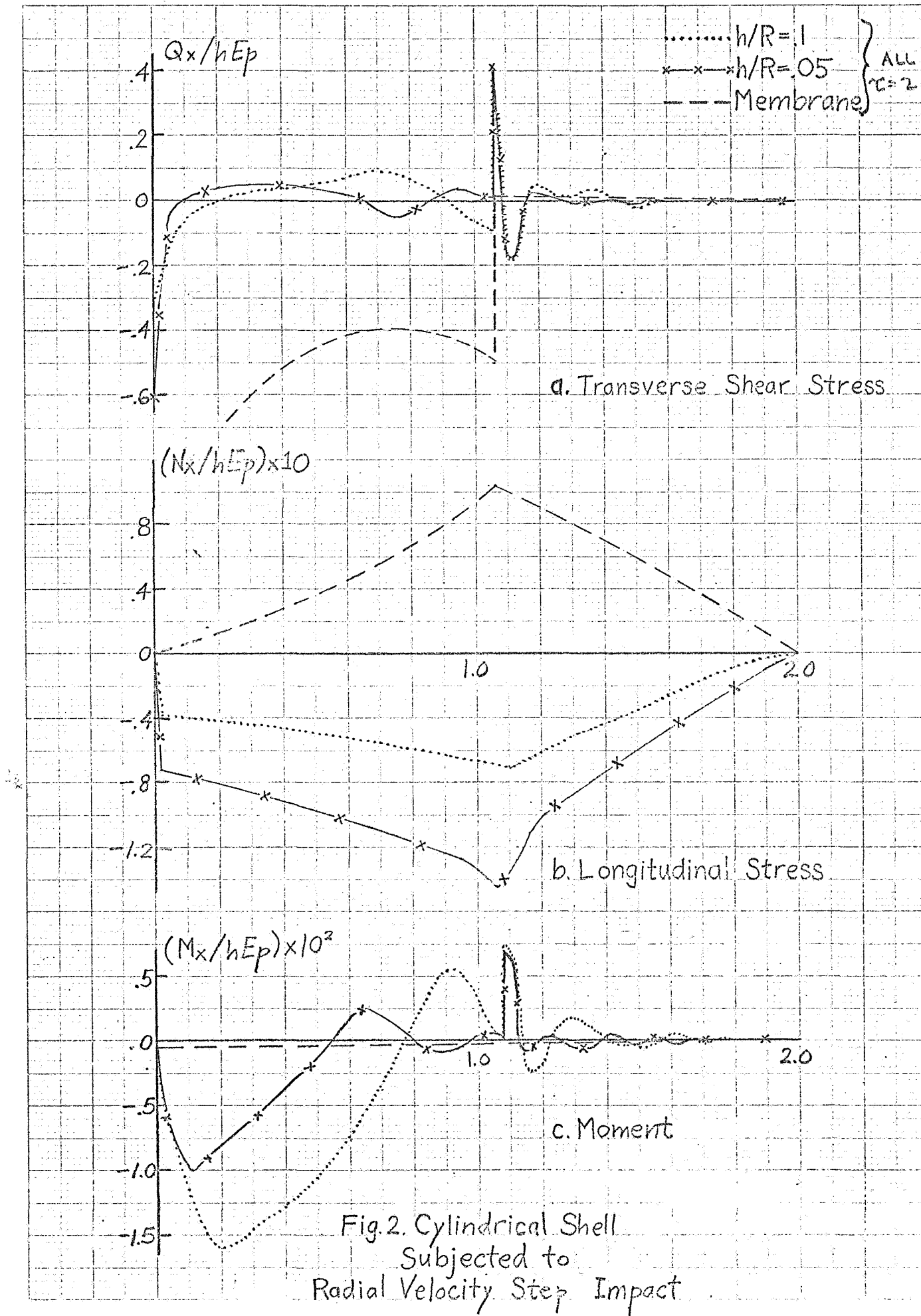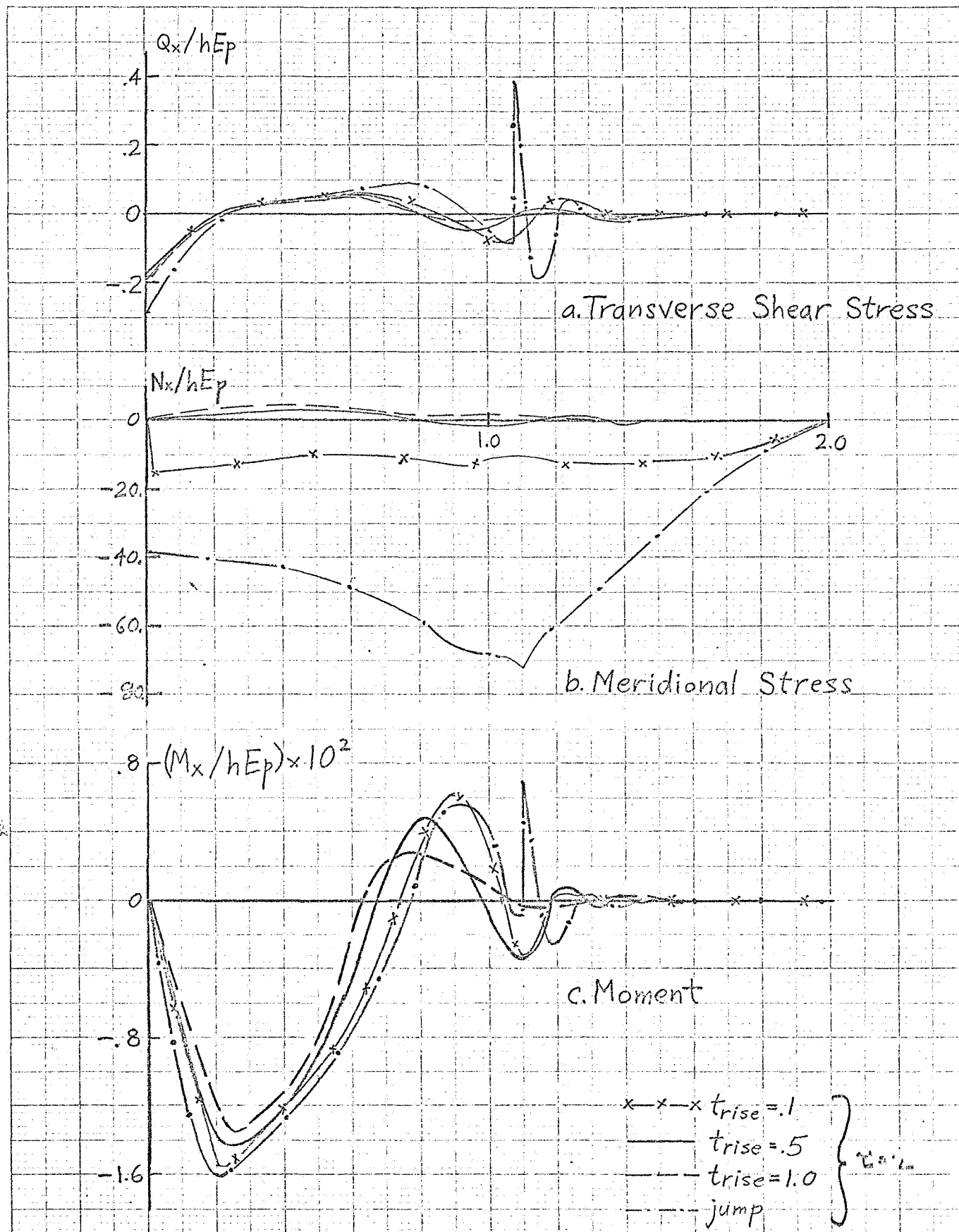
Fig. 3. Cylindrical Shell
Subjected to
Longitudinal Velocity Ramp Impact

-23-

Fig. 4. Cylindrical Shell
Subjected to
Longitudinal Velocity Ramp Impact

Fig. 5. Conical Shell
Subjected to
Longitudinal Velocity Step Impact

a. Transverse Shear Stress

b. Longitudinal Stress
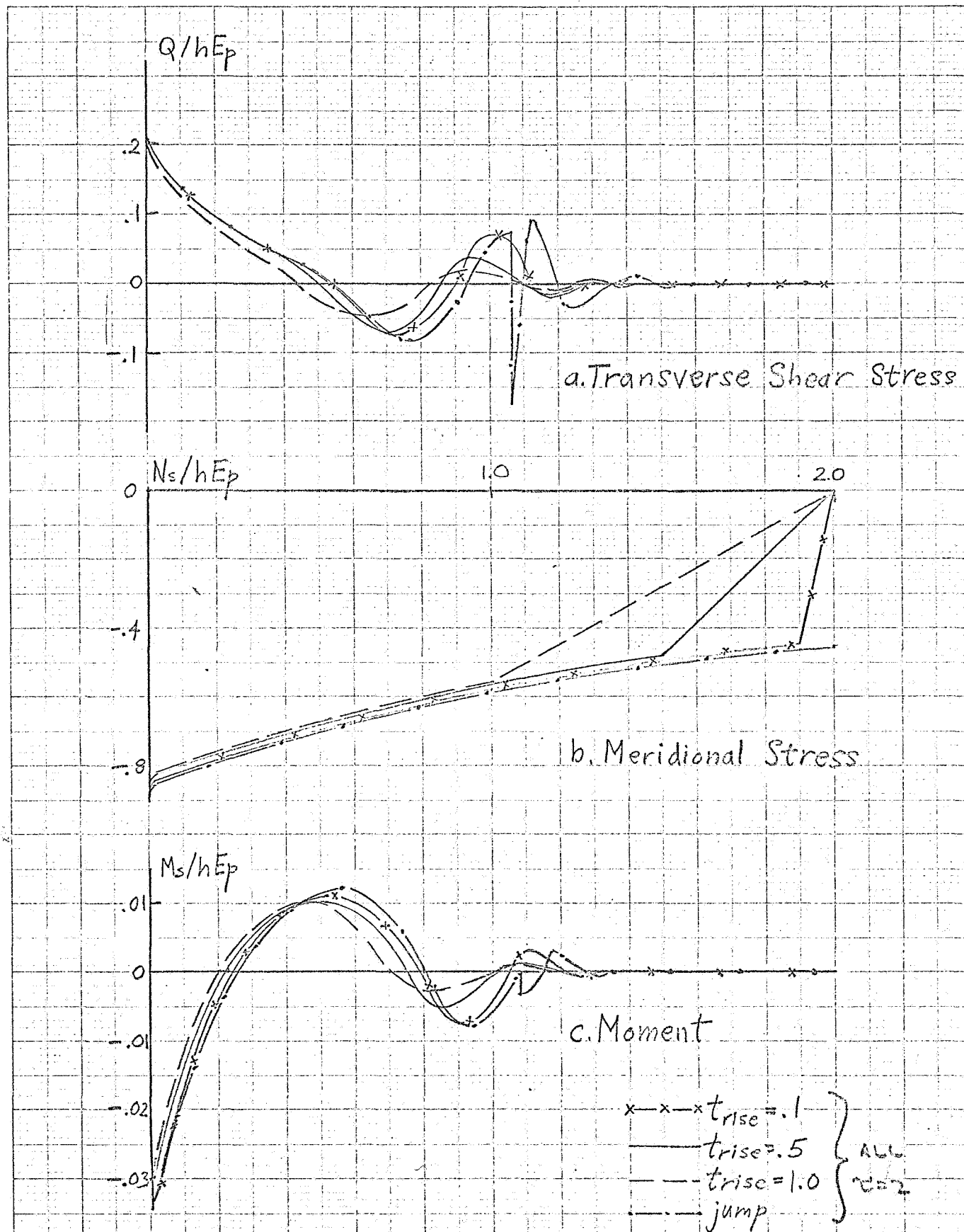
c. Moment
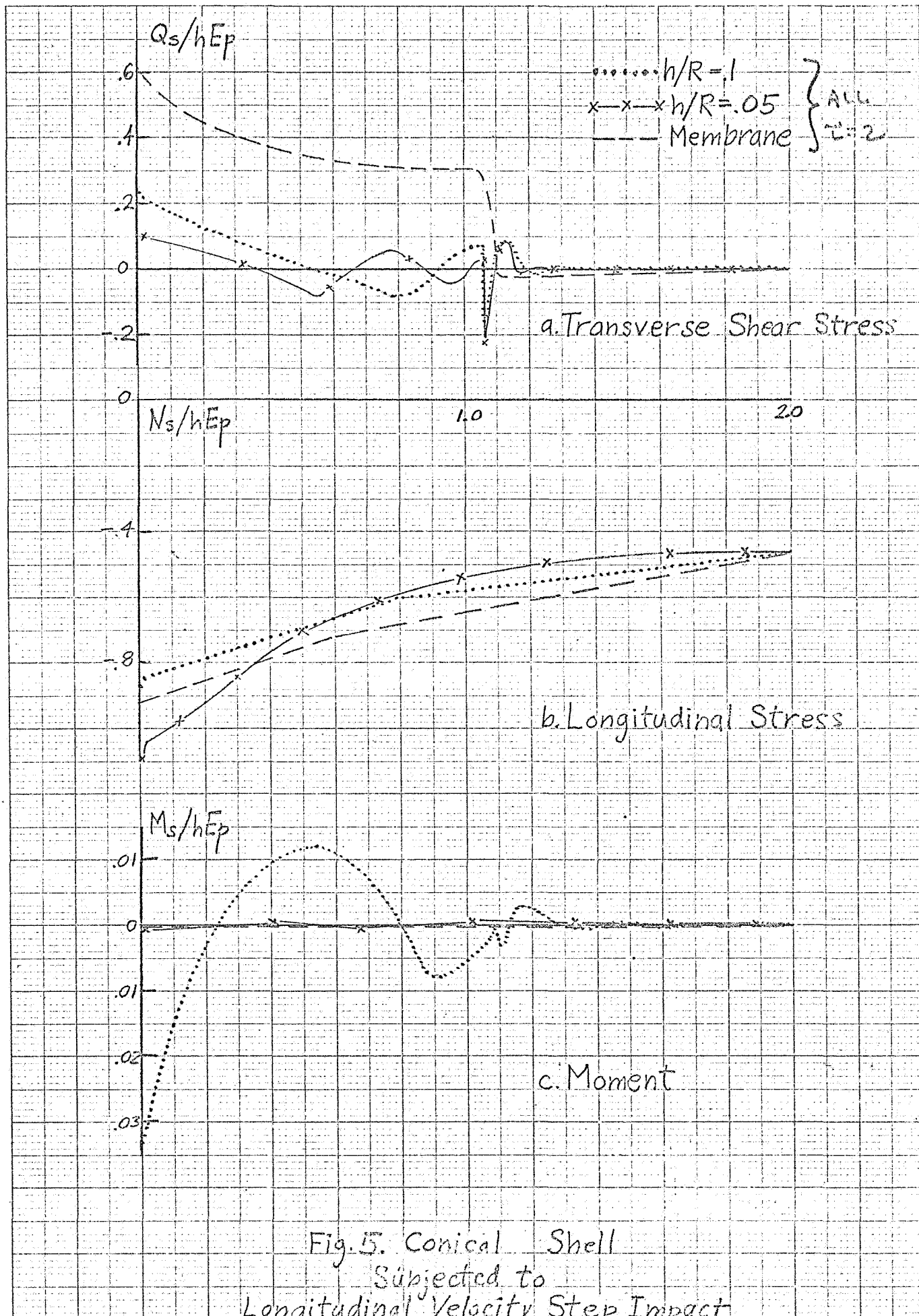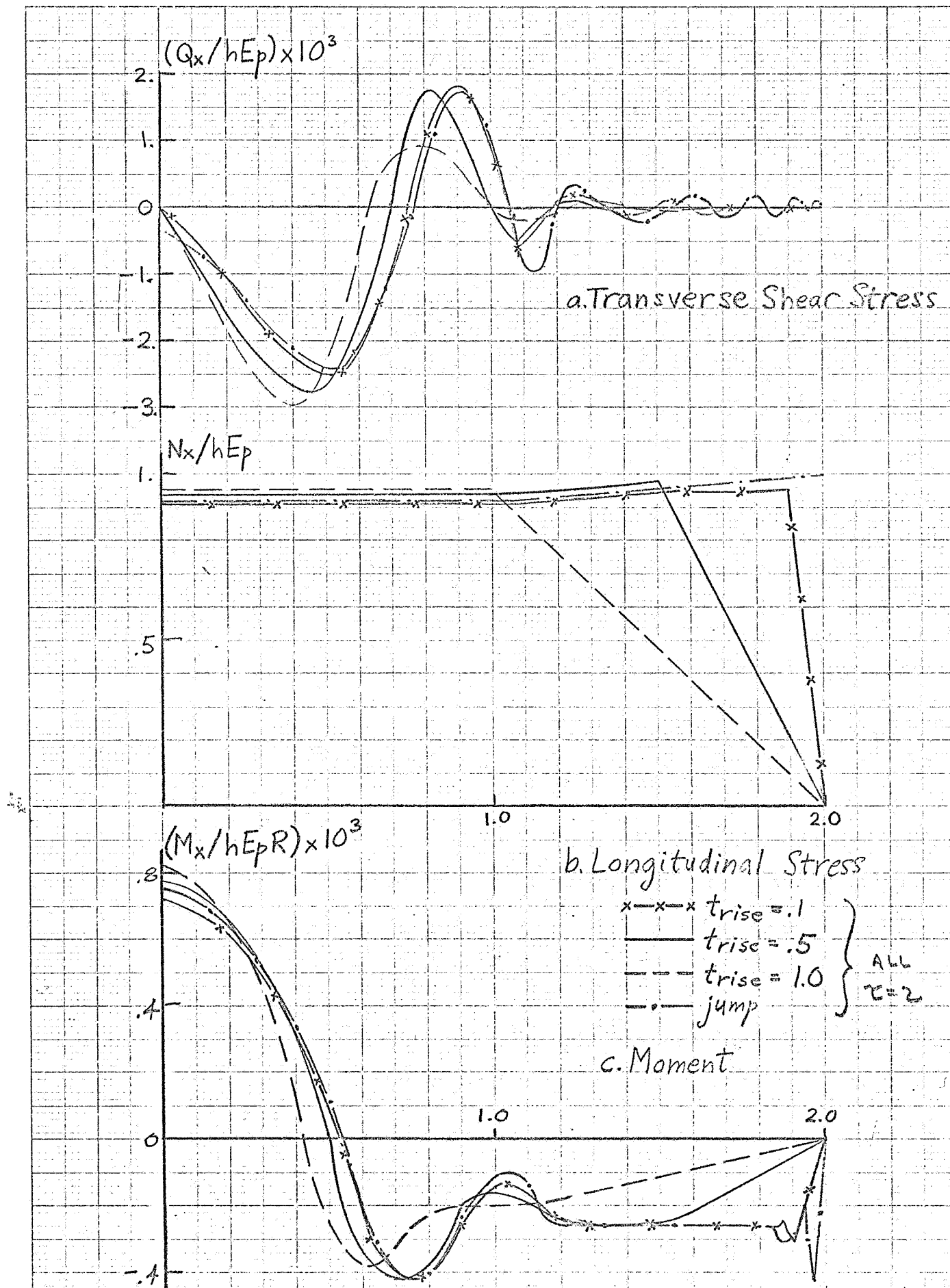
Fig. 6. Conical Shell Subjected to Longitudinal Velocity Ramp Impact
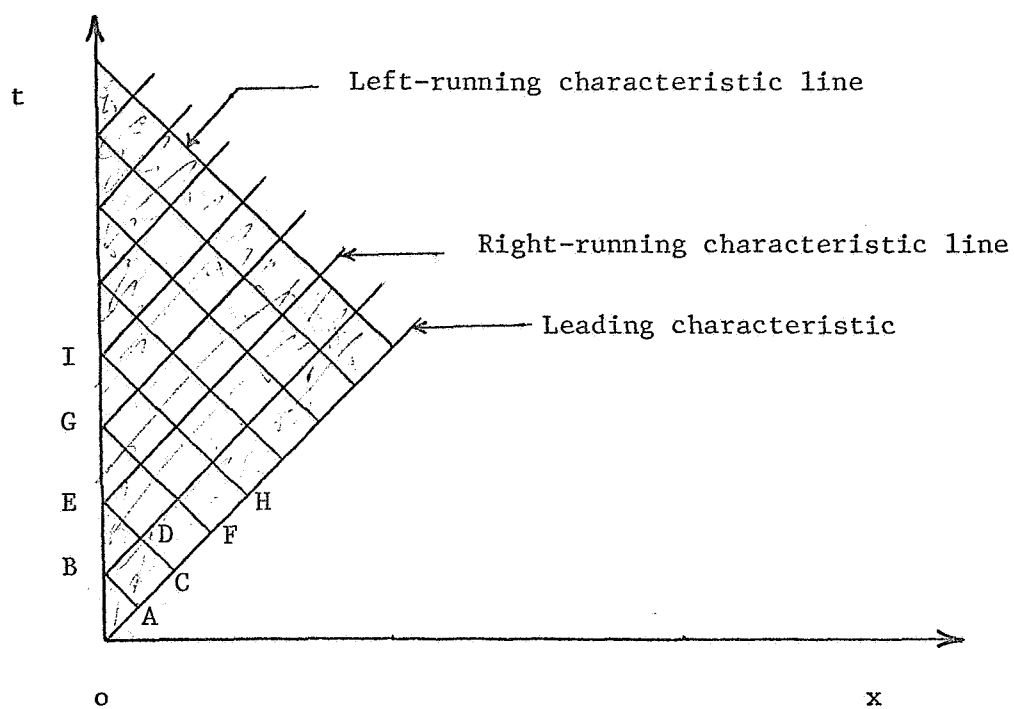
Figure 7 - Physical Plane (MCDIT-21)
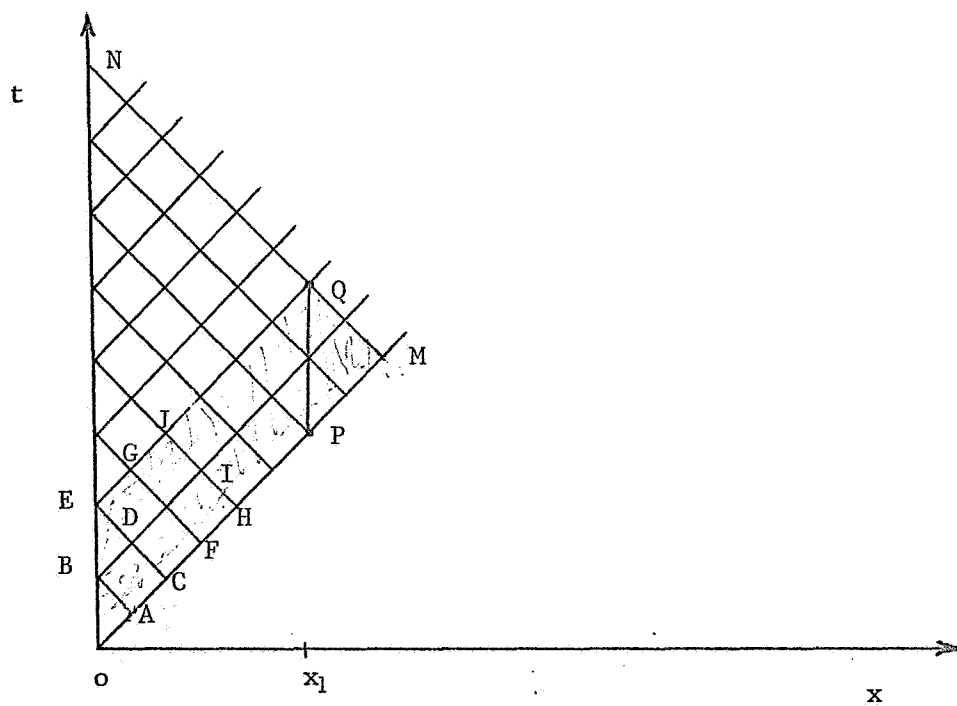
Figure 8 - Physical Plane (Modified MCDIT-21)

Pendulum → Arm

Shell Impacter →

Cardboard Tab →

Photodiodes

1 2 3

Slit Openings

1.48 cm.

FRONT VIEW

l_1

l_2

l_1 = distance to centerline of impact specimen

l_2 = distance to photodiode

Photodiodes →

Light source
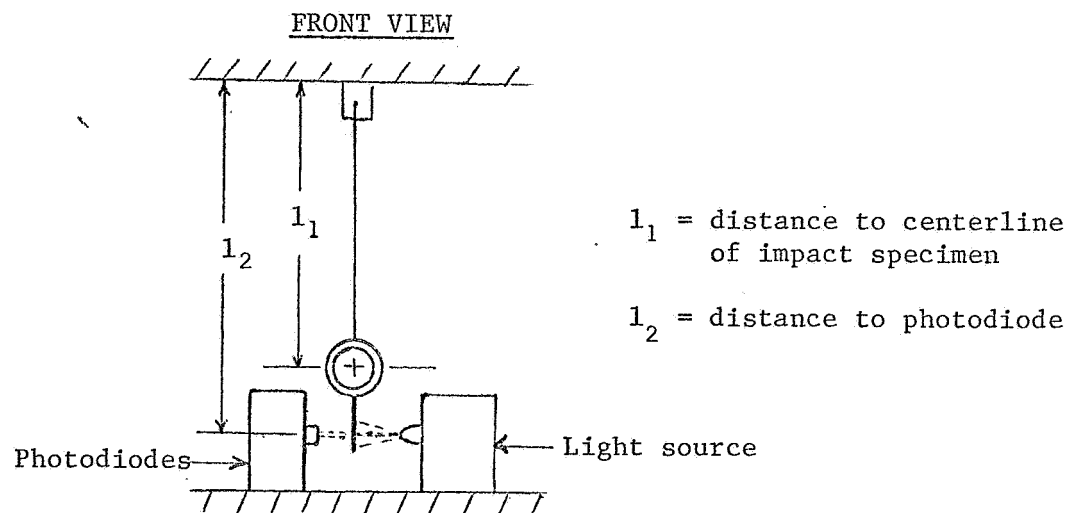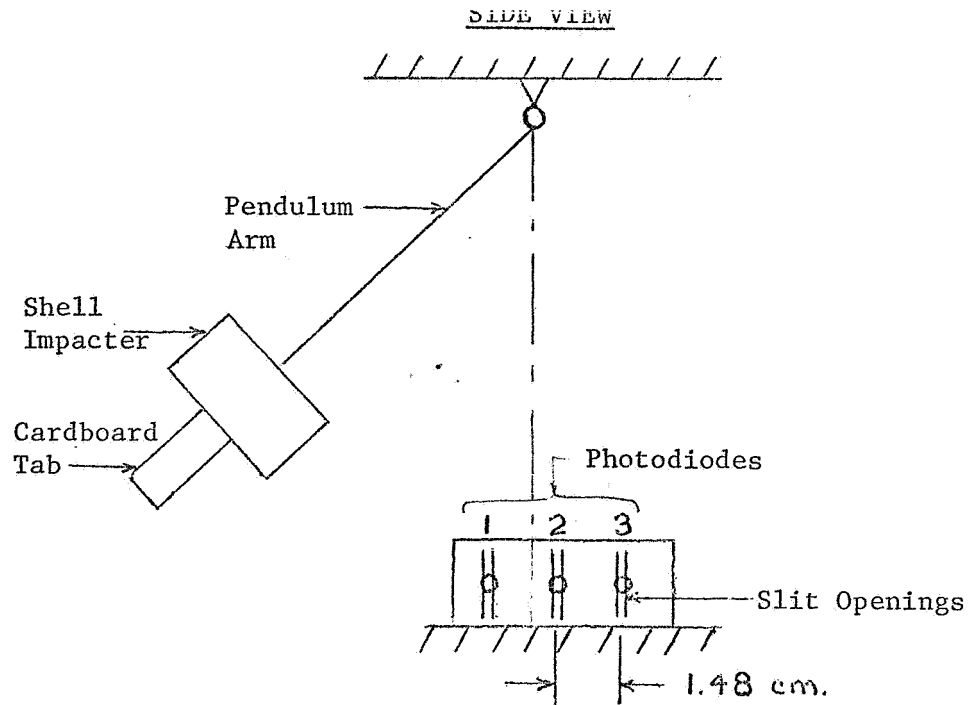
Figure 9. Photodiode System
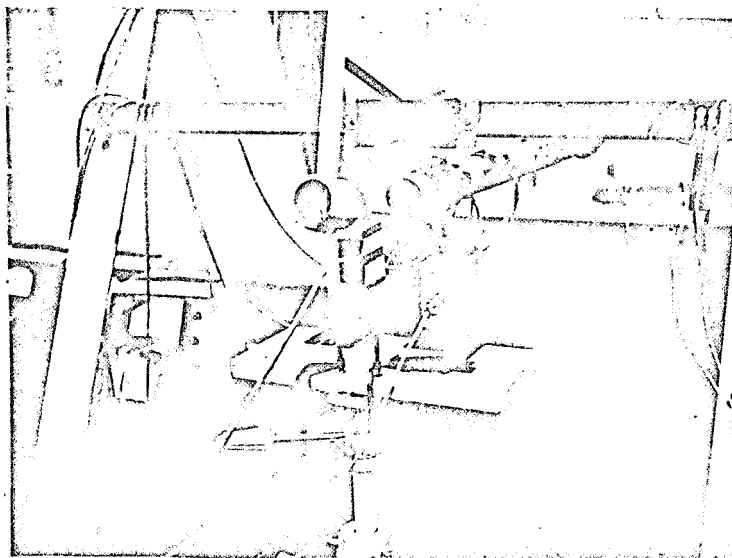
Figure 10. Photograph of Photodiode System

Interruption of Signal by Leading
Edge of Tab

Photograph of
Oscilloscope Screen

Sweep for Photodiode 2

Sweep for Photodiode 3

Time for Tab to Pass from Photodiode 2 to 3
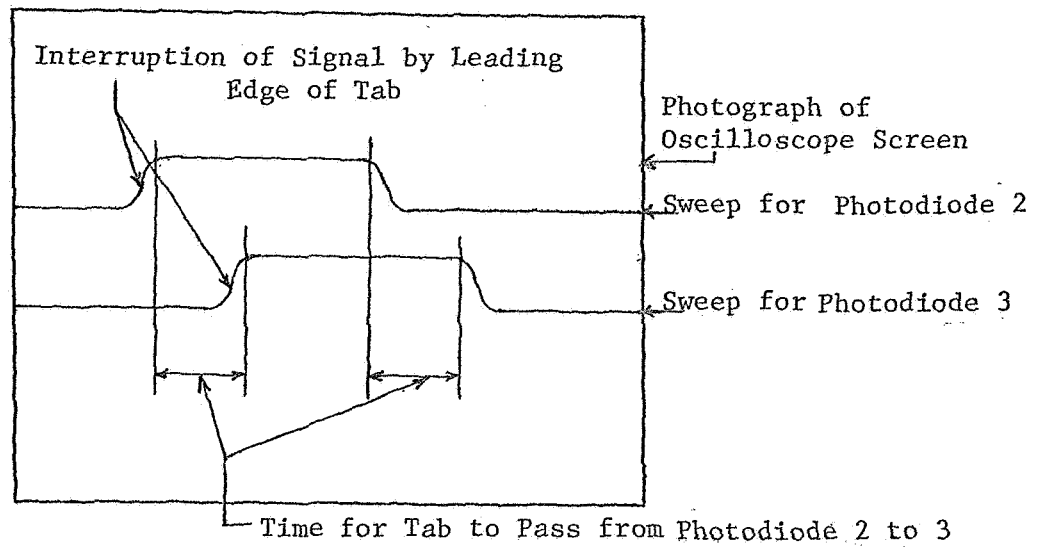
Figure II. Sketch of Photodiode Traces

Sweep for Photodiode I

Sweep for Photodiode 2

Sweep for Photodiode 3
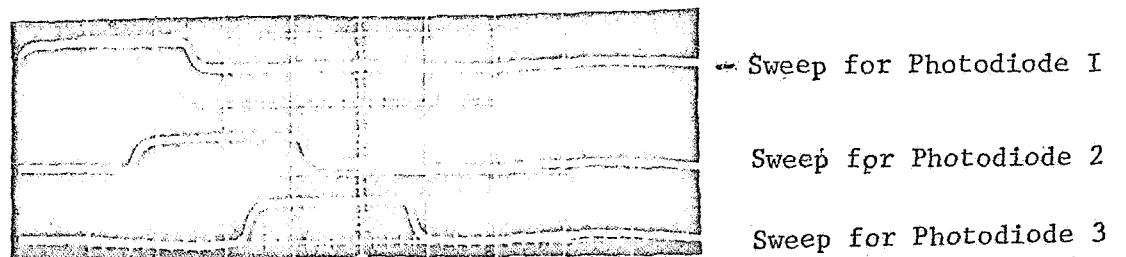
1 Millisecond / division

Figure 12. Photograph of Photodiode Traces
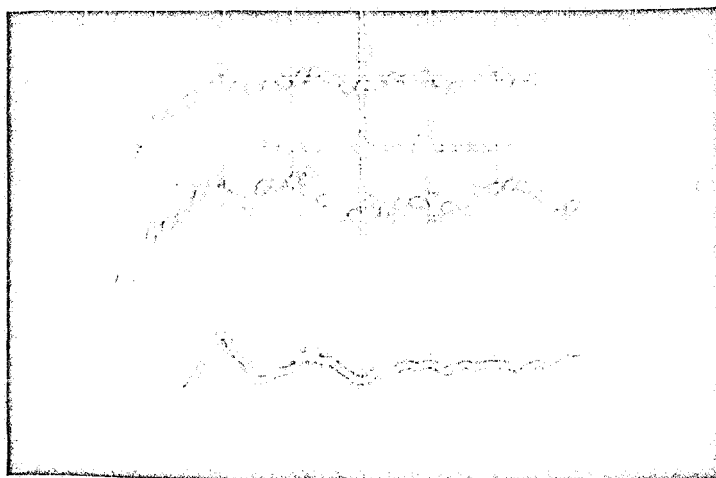
Figure 13   Simultaneity Oscilloscope Traces
(h/R = 0.133)
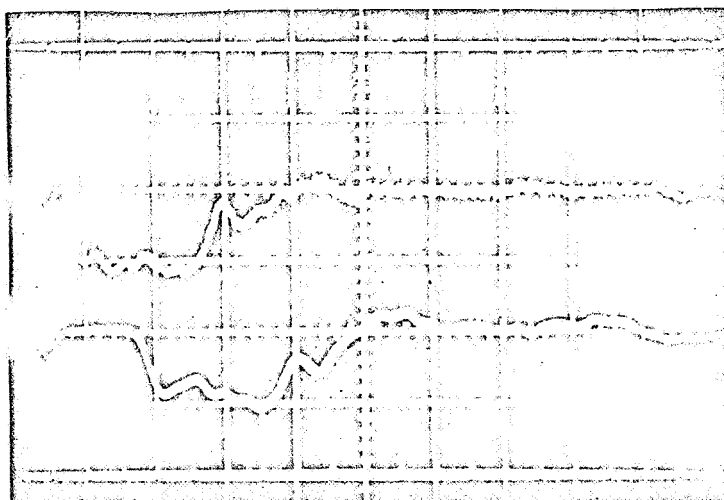
Figure 14   Longitudinal Strain Traces at 1" and 3"
(h/R = 0.286)
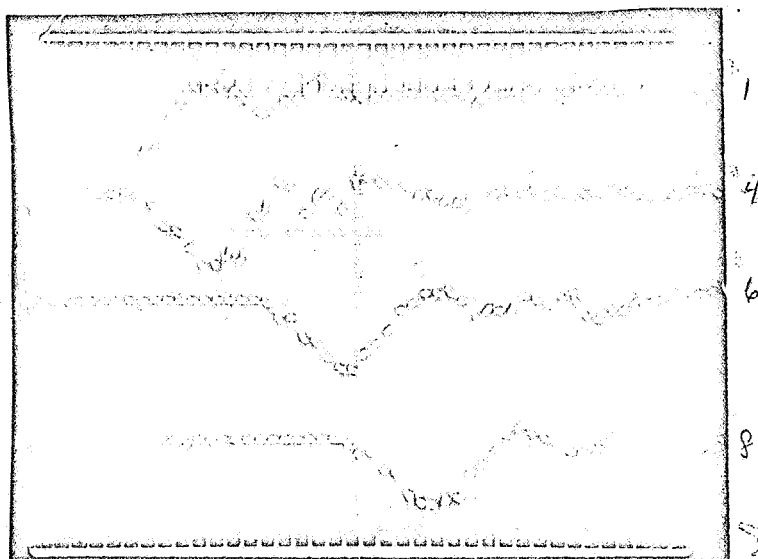
Figure 15   Longitudinal Strain Traces at 3", 7.5", 15", and 20"
(h/R = 0.286)

Scale

Gage 5 (Circum.)

200 μ in/in/cm

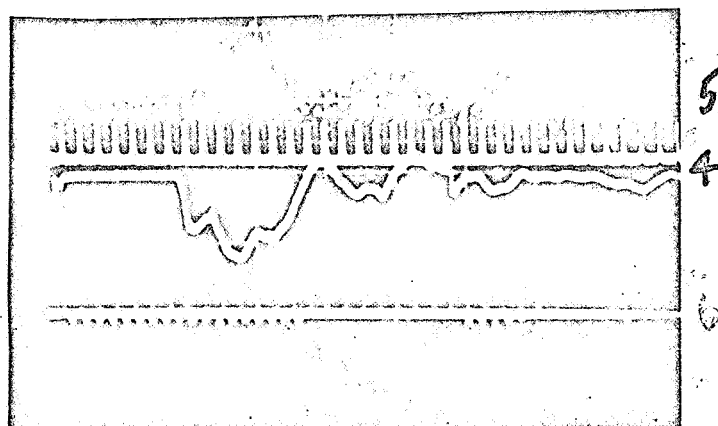20 μ sec/cm

Gages 4 and 6 (Long.)

400 μ in/in/cm

20 μ sec/cm

Figure 16   Circumferential and Longitudinal Strain Traces
(h/r = 0.052)

Scale

Gage 5 (Circum.)

200 μ in/in/cm

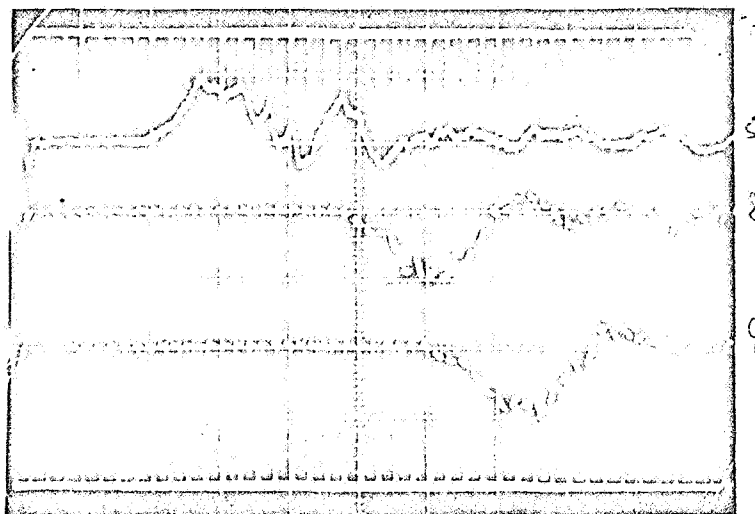20 μ sec/cm

Gages 8 and 9 (Long

400 μ in/in/cm

20 μ sec/cm

Figure 17   Circumferential and Longitudinal Strain Traces
(h/R = 0.286)
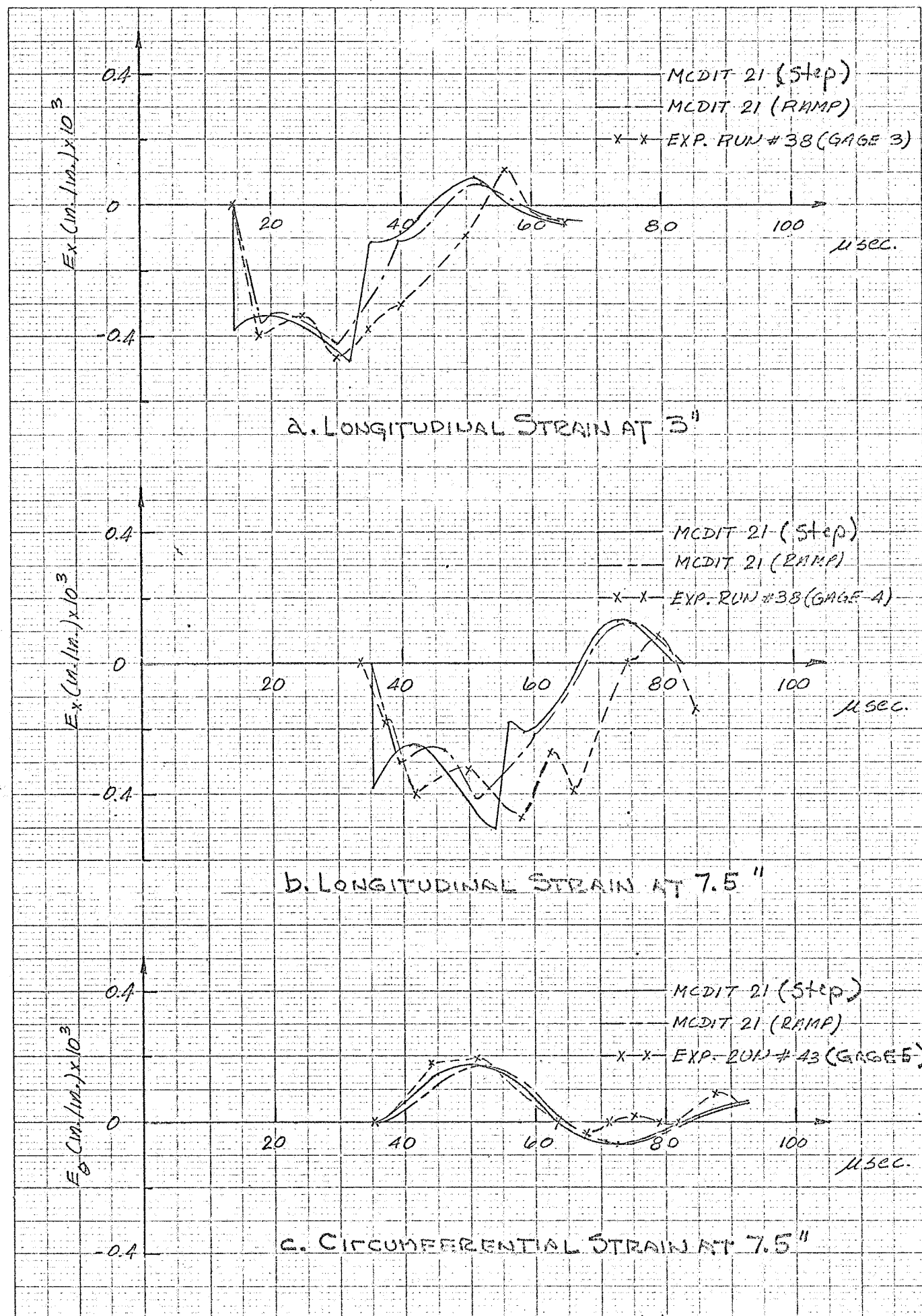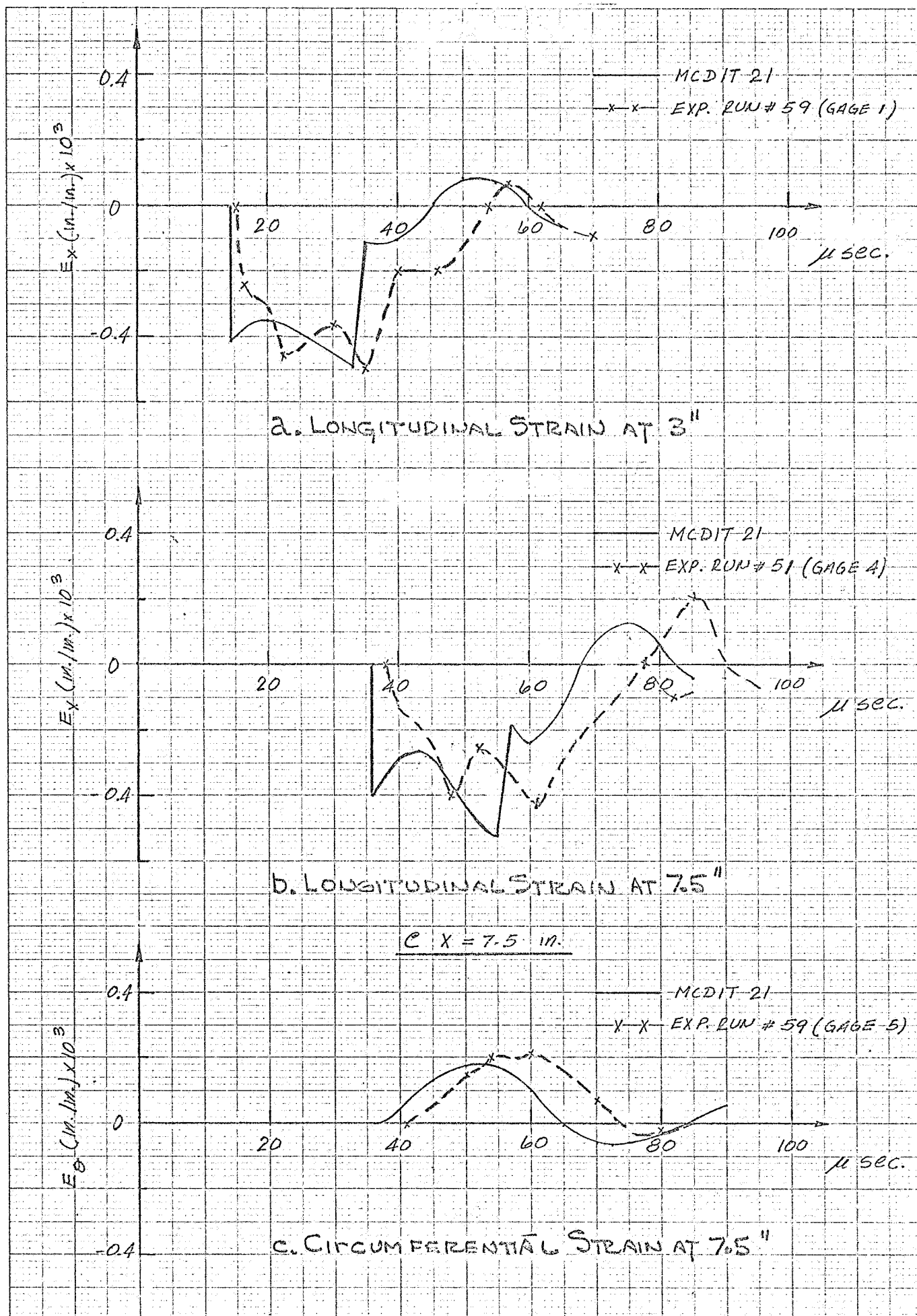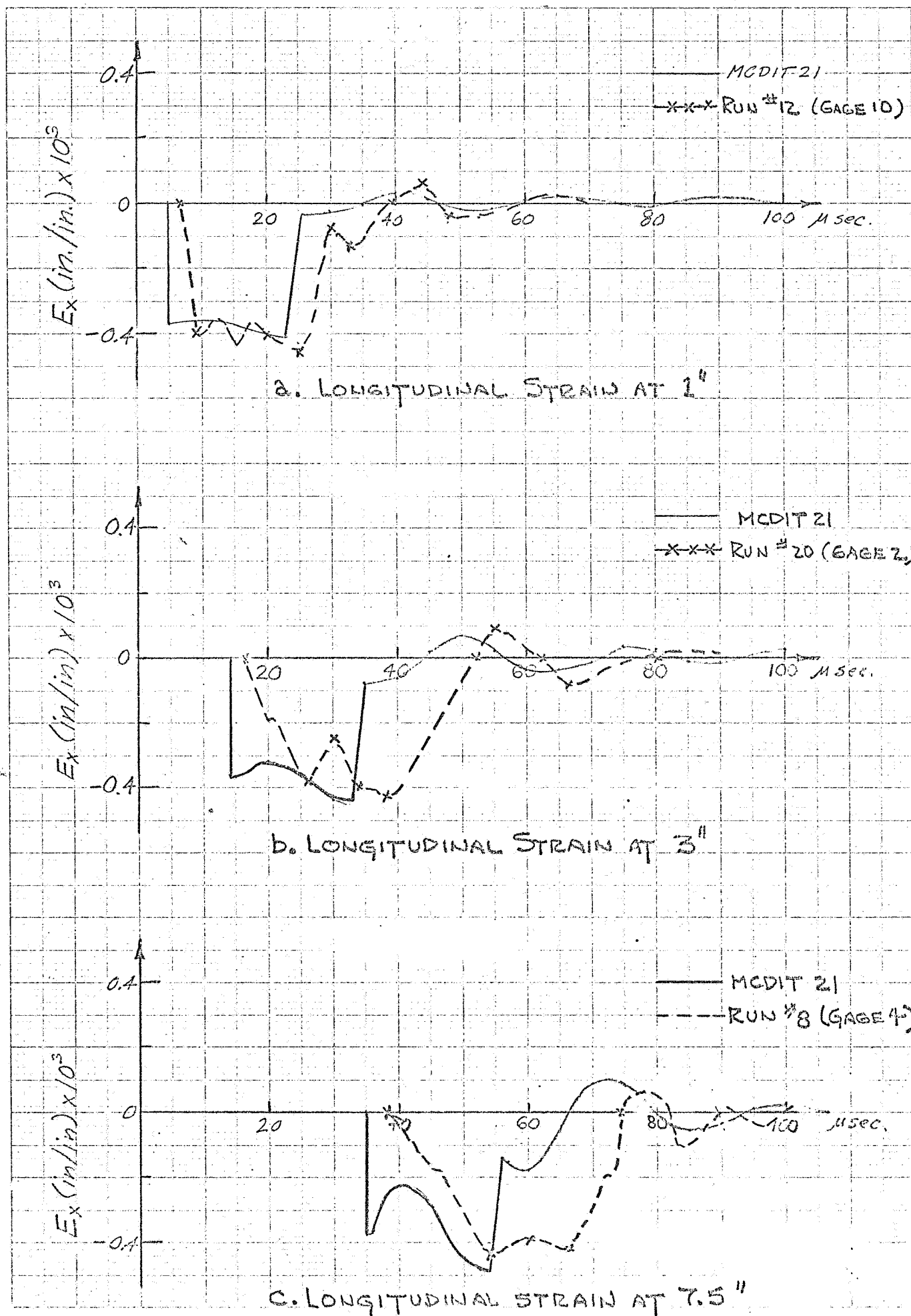
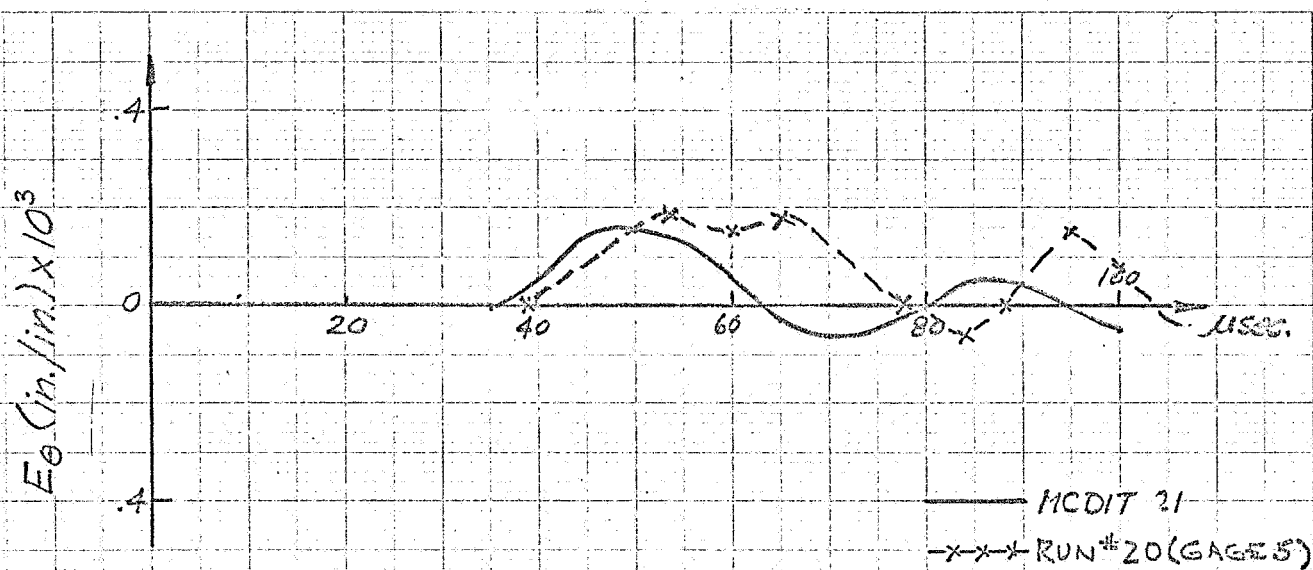a. LONGITUDINAL STRAIN AT 3"

b. LONGITUDINAL STRAIN AT 7.5"

c. CIRCUMFERENTIAL STRAIN AT 7.5"

FIGURE 18 STRAIN COMPARISONS OF h/R=0.052 SHELL

a. LONGITUDINAL STRAIN AT 3"

b. LONGITUDINAL STRAIN AT 7.5"

C X = 7.5 in.

c. CIRCUMFERENTIAL STRAIN AT 7.5"

FIGURE 19 STRAIN COMPARISONS OF h/R = 0.133 SHELL

a. LONGITUDINAL STRAIN AT 1"

b. LONGITUDINAL STRAIN AT 3"

c. LONGITUDINAL STRAIN AT 7.5"

FIGURE 20   -35-

d. Circumferential Strain at 7.5"

Figure 20 Strain Comparisons of h/R = 0.286 Shell
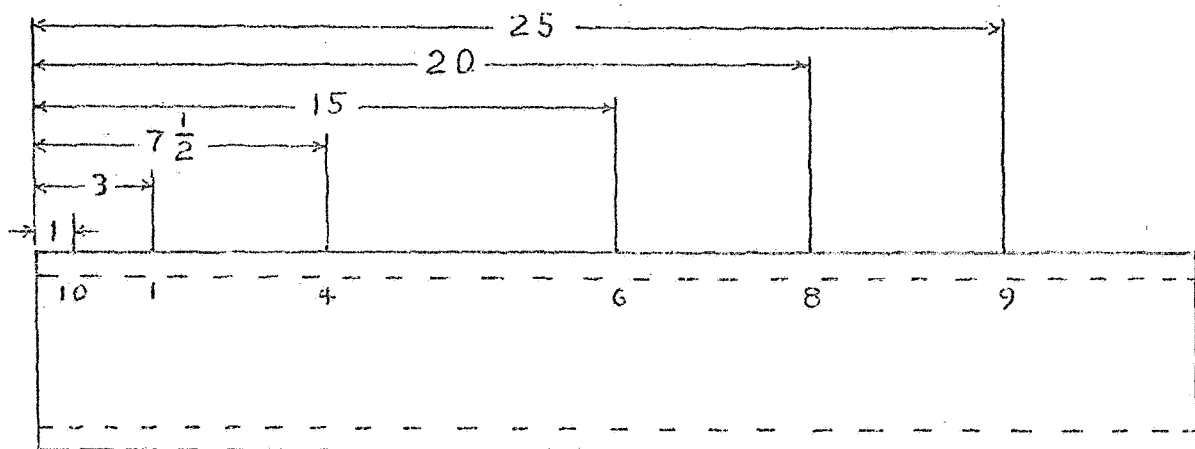
Ratio of Experimental Wave Speed to Theoretical Plate Velocity in ft/sec.

Specimen No.	10→1	1→4	4→6	6→8	8→9
T-1	‑‑‑‑‑	1.04	.96	.97	.98
T-13	.98	1.02	1.03	.99	1.04
T-14	1.06	1.02	1.00	1.00	.98

Specimen Material Properties (weight = 170.27 lb/ft³)

Specimen No.	h/R	E lb/in²	γ	C_plate ft/sec	C_dil ft/sec
* T-1	.052	10.34×10^6	.33	17,767	20,415
* T-13	.133	9.782×10^6	.33	17,281	19,842
** T-14	.286	10.25×10^6	.33	17,674	20,308

* Material properties measured
** Material properties estimated from various tensile samples.

TABLE 1 – WAVE VELOCITY COMPARISONS